



**HAL**  
open science

## **SILK studies - capturing the turnover of proteins linked to neurodegenerative diseases**

Ross Paterson, Audrey Gabelle, Brendan Lucey, Nicolas Barthelemy, Claire Leckey, Christophe Hirtz, Sylvain Lehmann, Chihiro Sato, Bruce Patterson, Tim West, et al.

### ► To cite this version:

Ross Paterson, Audrey Gabelle, Brendan Lucey, Nicolas Barthelemy, Claire Leckey, et al.. SILK studies - capturing the turnover of proteins linked to neurodegenerative diseases. *Nature Reviews Neurology*, 2019, 15 (7), pp.419-427. 10.1038/s41582-019-0222-0 . hal-02505307

**HAL Id: hal-02505307**







**<https://hal.science/hal-02505307>**

Submitted on 11 Mar 2020

**HAL** is a multi-disciplinary open access archive for the deposit and dissemination of scientific research documents, whether they are published or not. The documents may come from teaching and research institutions in France or abroad, or from public or private research centers.

L'archive ouverte pluridisciplinaire **HAL**, est destinée au dépôt et à la diffusion de documents scientifiques de niveau recherche, publiés ou non, émanant des établissements d'enseignement et de recherche français ou étrangers, des laboratoires publics ou privés.

# SILK studies — capturing the turnover of proteins linked to neurodegenerative diseases

Ross W. Paterson , Audrey Gabelle, Brendan P. Lucey, Nicolas R. Barthélemy, Claire A. Leckey, Christophe Hirtz, Sylvain Lehmann, Chihiro Sato , Bruce W. Patterson, Tim West , Kevin Yarasheski, Jonathan D. Rohrer, Norelle C. Wildburger , Jonathan M. Schott , Celeste M. Karch , Selina Wray, Timothy M. Miller, Donald L. Elbert, Henrik Zetterberg, Nick C. Fox and Randall J. Bateman

**Abstract** | Alzheimer disease (AD) is one of several neurodegenerative diseases characterized by dysregulation, misfolding and accumulation of specific proteins in the CNS. The stable isotope labelling kinetics (SILK) technique is based on generating amino acids labelled with naturally occurring stable (that is, nonradioactive) isotopes of carbon and/or nitrogen. These labelled amino acids can then be incorporated into proteins, enabling rates of protein production and clearance to be determined *in vivo* and *in vitro* without the use of radioactive or chemical labels. Over the past decade, SILK studies have been used to determine the turnover of key pathogenic proteins amyloid- $\beta$  (A $\beta$ ), tau and superoxide dismutase 1 (SOD1) in the cerebrospinal fluid of healthy individuals, patients with AD and those with other neurodegenerative diseases. These studies led to the identification of several factors that alter the production and/or clearance of these proteins, including age, sleep and disease-causing genetic mutations. SILK studies have also been used to measure A $\beta$  turnover in blood and within brain tissue. SILK studies offer the potential to elucidate the mechanisms underlying various neurodegenerative disease mechanisms, including neuroinflammation and synaptic dysfunction, and to demonstrate target engagement of novel disease-modifying therapies.

The accumulation of misfolded proteins in the CNS is a pathogenetic mechanism shared by several neurodegenerative diseases, including Alzheimer disease (AD), Parkinson disease and some forms of dementia. Understanding the mechanisms and rates of production and clearance for specific proteins associated with these diseases will be important to understand how such a state of disequilibrium arises and to identify the factors that influence it.

Naturally occurring stable isotopes of chemical elements, such as  $^{13}\text{C}$ ,  $^{15}\text{N}$  and  $^2\text{H}$ , have been used to interrogate human physiology and pathophysiology since

their discovery in the 1920s<sup>1</sup>. However, such isotopes have been employed to probe protein synthesis and clearance rates in the CNS *in vivo* and *in vitro* only during the past decade. The isotopes used in stable isotope labelling kinetics (SILK) studies possess additional neutrons in their atomic nuclei that make them fractionally heavier but nonradioactive. As these isotopes are chemically identical to the natural element, they participate in the same reactions and become incorporated into organic molecules such as proteins and DNA. Mass spectroscopy (MS) can be used to distinguish isotope-labelled compounds from their unlabelled counterparts on the

basis of their mass difference. As these ‘heavy’ isotopes do occur in nature, albeit at very low concentrations, all organic molecules will demonstrate a background level of incorporation that must be considered in the analysis.

Amino acids labelled with stable isotopes can be administered to humans either intravenously or orally, becoming incorporated into (and thereby labelling) newly translated proteins. These labelled proteins are harvested from blood, cerebrospinal fluid (CSF) and/or tissue samples and are typically enriched by immunoprecipitation before being digested using enzymes such as trypsin, LysN or AspN proteases. The ratio of labelled to nonlabelled peptide, which can be quantified using targeted MS, reflects the rate of labelled amino acid incorporation into the protein. Thus, SILK studies can provide dynamic measures of protein synthesis, protein release into body fluids or tissue and protein clearance. Furthermore, SILK has the potential to provide immediate *in vivo* evidence of target engagement in clinical trials, thereby advancing therapeutic discovery.

Alternative ways to measure protein turnover (for example, using radioactive isotopes such as  $^{35}\text{S}$ -methionine) have been used to determine protein kinetics in *in vitro* systems. However, radioactive isotopes have limited use in humans, create substantial laboratory overheads when used for *in vitro* studies and (unlike SILK) cannot provide highly specific and precise turnover data on individual proteins. Proteins can also be chemically tagged with a variety of optical and other molecules for tracking turnover and transport<sup>2</sup>. These systems are widely used *in vitro*; however, they all have limited applicability in humans or animal models, and the label itself can also potentially influence protein kinetics. By contrast, SILK studies essentially label proteins subatomically (that is, with additional neutrons), which avoids the risk of artefactually altering protein kinetics. The SILK technique has been proved safe in animal and human studies.

In this Perspectives article, we discuss the principles of SILK, summarize the results of key studies in which SILK provided insights into neurodegenerative disease and discuss its utility across clinical and preclinical models of these diseases.

**Principles of SILK**

SILK has been used in preclinical model systems, including induced pluripotent stem cells (iPSCs), cell culture and animal models, as well as in humans, to measure protein synthesis and clearance rates (FIG. 1). The SILK method involves administration of essential amino acids (that is, indispensable amino acids that cannot be synthesized by the body) enriched with naturally occurring stable isotopes; accordingly, the incorporation of these amino acids into newly synthesized proteins gradually

increases until a steady state is reached. After administration of the labelled amino acid stops, the proportion of the labelled amino acid in the target protein gradually declines owing to protein clearance or degradation. Changes in the isotopic enrichment of the target protein enable the calculation of protein synthesis and clearance rates from the ratio of labelled (heavy) to nonlabelled (light) protein (FIG. 1).

Leucine labelled with six  $^{13}\text{C}$  atoms ( $^{13}\text{C}_6$ -leucine) is the most widely used amino acid in SILK studies to date.

Most in vitro and in vivo biological systems cannot discriminate  $^{13}\text{C}_6$ -labelled amino acids from  $^{12}\text{C}_6$  amino acids, and, similarly, the heavy nitrogen isotope  $^{15}\text{N}$  cannot be distinguished from native  $^{14}\text{N}$ . Therefore, the incorporation of  $^{13}\text{C}_6$ -leucine into newly synthesized proteins follows identical pathways and kinetics to those of  $^{12}\text{C}_6$ -leucine<sup>3</sup>. When  $^{13}\text{C}_6$ -leucine is administered, each successive leucine in the target protein is incorporated as either  $^{13}\text{C}_6$ -leucine or  $^{12}\text{C}_6$ -leucine. MS can then be applied to tissue or biofluid samples to identify and quantify these two forms. Kinetic models of the system are then used to estimate in vivo protein production, aggregation, transport and degradation rates.

By way of example, amyloid- $\beta$  (A $\beta$ ) is produced primarily by neurons in the brain and is then secreted into the CSF<sup>4</sup>. As A $\beta$  peptides in the CNS are continually being produced, degraded and cleared, the turnover of A $\beta$  is the sum total of all the mechanisms underlying its accumulation, aggregation and removal. Irreversible deposition into amyloid plaques removes A $\beta$  from the interstitial fluid (ISF), but not from the CNS. A $\beta$  clearance from the CNS can occur via ISF or CSF transport, resorption<sup>5</sup>, transport across the blood-brain barrier<sup>6</sup>, reuptake by brain tissue, in situ proteolysis<sup>7</sup> and glymphatic clearance<sup>8</sup>. Through serial sampling of blood and CSF, SILK can be used to investigate these processes. When a stable isotope-labelled amino acid (tracer) is introduced, the isotopic enrichment (that is, the abundance) of heavy A $\beta$  peptides increases over time as unlabelled peptides are replaced by newly synthesized, isotope-labelled peptides (Supplementary Movies 1–3). After tracer administration is discontinued, isotopic enrichment of the target protein or peptide gradually declines towards its natural (negligible) abundance. SILK can similarly be used to measure the kinetics of a variety of other important neuronal proteins, including tau, superoxide dismutase 1 (SOD1) and  $\alpha$ -synuclein; as rates of protein synthesis and clearance differ, specific labelling protocols need to be established for each protein of interest.

Compartmental models can provide a mathematical framework that describes the flow of tracer from the administration site to the locus of protein synthesis and finally into the sampled tissue or fluid. In the case of A $\beta$ , tracer is introduced into blood and incorporated into A $\beta$  in the CNS and is sampled in CSF (FIG. 2; Supplementary Movie 3). The model's structure and rate constants affect the shape and magnitude

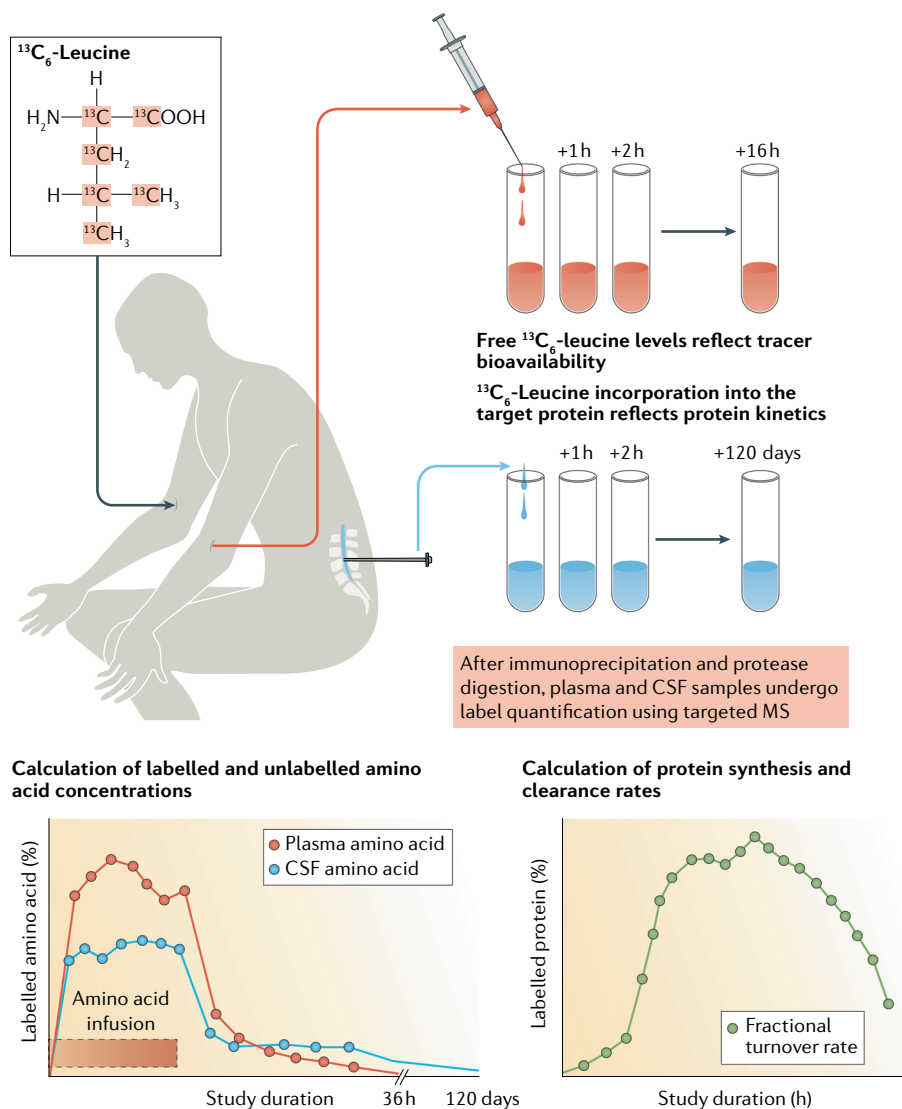


**Fig. 1 | Stable isotope labelling kinetics methodology.** Stable isotope labelling kinetics (SILK) studies in humans involve infusion of an amino acid labelled with a stable isotope, such as  $^{13}\text{C}$ -leucine. To measure the turnover rate of a specific protein of interest, blood and cerebrospinal fluid (CSF) samples are collected at baseline and at appropriate intervals thereafter. Sampling intervals and duration are determined by the protein turnover rate.  $^{13}\text{C}$ -Leucine levels in blood reflect tracer bioavailability, whereas  $^{13}\text{C}$ -leucine levels in CSF and/or other body fluids reflect tracer incorporation into the target protein. To determine target protein kinetics, CSF samples usually undergo immunoprecipitation (to achieve target protein enrichment) and protease digestion, followed by label quantification using targeted mass spectrometry (MS). These data are used to calculate the concentrations of labelled and unlabelled protein and, in compartmental modelling studies, to determine protein turnover rates.

of the predicted enrichment time course and curves are adjusted to optimize their fit to the observed SILK data. The labelling data are transformed by the model into a set of parameters that can be used to determine the effect of factors such as age<sup>9</sup>, sex, *APOE4* genotype<sup>10</sup>, autosomal dominant AD (ADAD)-related mutation status<sup>11</sup>, drug treatment<sup>12</sup>, sleep<sup>13</sup> and amyloid deposition status<sup>9</sup> on A $\beta$  kinetics.

### Applying SILK to key proteins

In this section, we summarize the major findings from SILK experiments to date, focusing on proteins linked to neurodegenerative diseases.

#### Amyloid- $\beta$

In order to measure A $\beta$  kinetics in the human CNS, a translational protocol was developed to label and track A $\beta$  over a 36 h period during and after a 9 h intravenous infusion of <sup>13</sup>C<sub>6</sub>-leucine<sup>9,14,15</sup>. This protocol was then applied to SILK studies of individuals with ADAD<sup>11</sup>, sporadic AD and unaffected controls<sup>9</sup> to measure the turnover of three A $\beta$  peptides — A $\beta$ 38, A $\beta$ 40 and A $\beta$ 42. A highly consistent finding in both ADAD and sporadic AD is that the turnover or clearance of soluble A $\beta$ 42 is specifically increased in individuals with amyloidosis, whereas A $\beta$ 38 and A $\beta$ 40 fractional turnover rates were unaltered by the presence of amyloidosis (FIG. 3). Furthermore, the A $\beta$ 42:A $\beta$ 40 turnover rate ratio was positively correlated with the amyloid plaque load, as measured by Pittsburgh compound B PET ( $r=0.45$ ), and with the amyloid plaque growth rate ( $r=0.75$ ), suggesting that faster turnover of A $\beta$ 42 represents increased deposition of A $\beta$ 42 relative to A $\beta$ 40 in amyloid plaques<sup>9,11</sup>. In addition, the A $\beta$ 42:A $\beta$ 40 production rate ratio was higher in *PSEN* mutation carriers than in non-carriers, which suggested that A $\beta$ 42 overproduction also contributes to ADAD. The turnover rates of all A $\beta$  peptides slowed substantially with increasing age (half-lives for all peptides increased by 2.5-fold between the ages of 30 years and 80 years)<sup>9</sup>, which might account for the observed age-related increase in the risk of amyloid accumulation.

SILK studies of A $\beta$  kinetics also enabled the mechanisms of action for proposed disease-modifying therapeutics to be investigated<sup>16</sup>. For example, treatment with  $\gamma$ -secretase and  $\beta$ -secretase 1 inhibitors resulted in a dose-dependent reduction in the accumulation of newly synthesized A $\beta$ <sup>12,17</sup>, without altering its clearance kinetics<sup>12</sup>. This observation implies that treatment with these agents

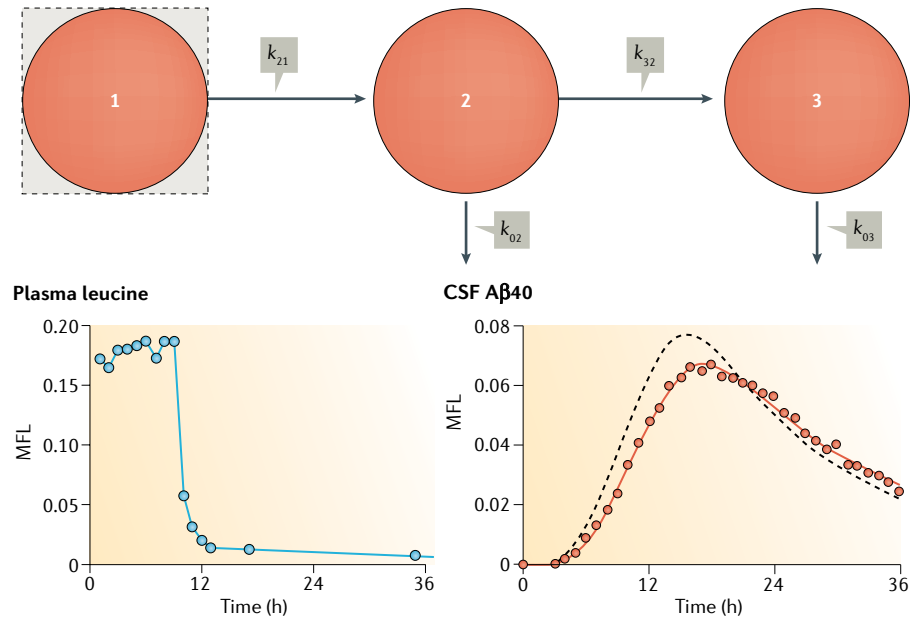


**Fig. 2 | Compartmental modelling of <sup>13</sup>C-leucine kinetics in humans.** In this hypothetical model, compartment 1 represents the <sup>13</sup>C-leucine tracer infusion site (typically blood) and compartment 2 represents the site of tracer incorporation into intermediates, such as amyloid precursor protein (APP), as well as transport delay processes. Compartment 3 represents the site of tracer incorporation into the protein of interest, such as amyloid- $\beta$  (A $\beta$ )40 in cerebrospinal fluid (CSF). The formula  $k_{xy}$  is used to calculate the fraction of compartment  $y$  converted to compartment  $x$  per unit time, where 0 represents loss from the system. This calculation transforms the plasma <sup>13</sup>C-leucine curve (left) into the A $\beta$ 40 <sup>13</sup>C-leucine curve (right). Mole fraction labelled (MFL) is a 'forcing function' that uses linear interpolation between measured time points to define tracer bioavailability for incorporation into target proteins. The compartmental model typically identifies a fractional turnover rate for the whole system, namely, the fraction of a rate-limiting compartment that is irreversibly removed per unit time. Mass flux rates along a pathway are calculated as the compartment mass multiplied by the rate constant. Specifically, if compartment 3 represents CSF A $\beta$ , then the flux of A $\beta$  through CSF (that is, the rate of appearance of A $\beta$  into and disappearance of A $\beta$  from CSF at steady state) is the product of the CSF concentration and  $k_{03}$ . Compartmental modelling of stable isotope labelling kinetics (SILK) data consists of constructing a physiologically plausible model with optimized rate constants that provides an excellent fit to the experimental A $\beta$ 40 SILK data (solid line). In the CSF A $\beta$ 40 SILK data shown, gross systematic errors in the fit would result if  $k_{03}$  is increased by 20% (dashed line).

reduces A $\beta$  production, leading to reduced accumulation of A $\beta$ . Moreover, SILK studies of plasma concentrations of A $\beta$  in patients with sporadic AD and healthy control participants demonstrated that, in both groups, turnover of A $\beta$  is about three times faster in plasma than in CSF<sup>18</sup>. Plasma A $\beta$ 42 and A $\beta$ 40 kinetics are virtually identical in individuals without amyloid deposition, whereas in amyloid-positive individuals (that is, those with substantial brain A $\beta$  accumulation), fractional turnover of A $\beta$ 42 is faster than that of A $\beta$ 40. The same pattern was observed in CSF, albeit with a smaller magnitude of difference<sup>18</sup>. The findings of these plasma A $\beta$  SILK studies led to the discovery that the plasma A $\beta$ 42:A $\beta$ 40 concentration ratio is a highly specific biomarker of brain amyloid plaques and elevated A $\beta$  levels in CSF<sup>18,19</sup>.

#### Effect of poor sleep on amyloid- $\beta$ kinetics.

In both mouse and human studies, the concentration of A $\beta$  in brain ISF and CSF oscillates with the sleep-wake cycle<sup>20,21</sup>. Because A $\beta$  deposition in the brain is concentration-dependent, prolonged bouts of wakefulness owing to sleep disturbances might increase the risk of AD via an A $\beta$ -mediated mechanism<sup>22</sup>. To determine the kinetics underlying this A $\beta$  oscillation, a SILK study found that the CSF concentration of A $\beta$  increased by ~30% during sleep deprivation, although A $\beta$  SILK curves in sleep-deprived individuals were similar to those of normal-sleep controls<sup>13,22</sup>. In the SILK model, changes in A $\beta$  production rate are directly proportional to CSF A $\beta$  concentration, whereas the shape of the SILK curves is most sensitive to changes in A $\beta$  clearance rates (Supplementary Movies 1,2). This observation suggests that

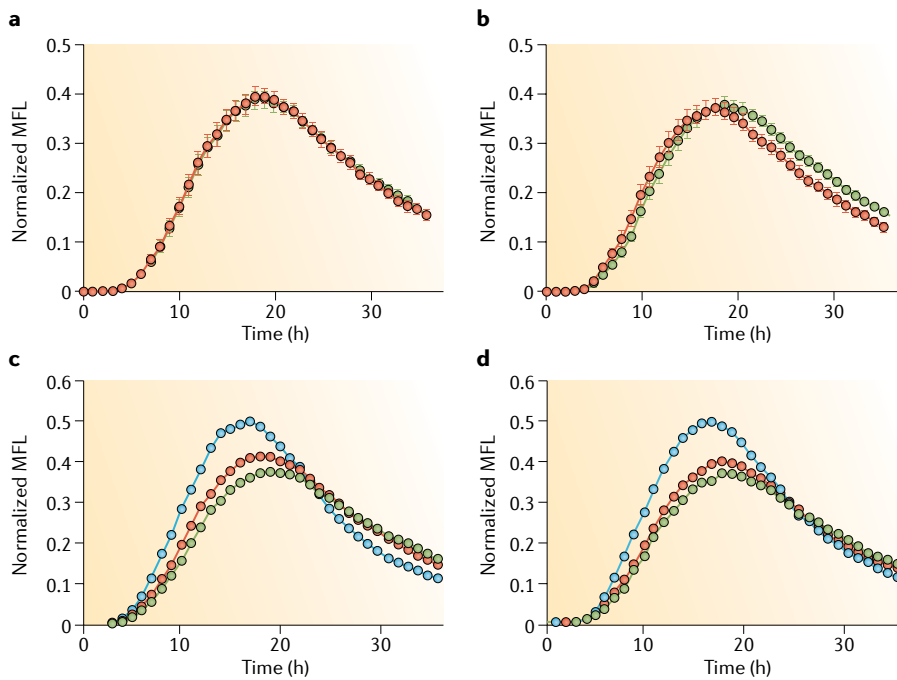


**Fig. 3 | Data from stable isotope labelling kinetics studies of amyloid- $\beta$  in humans.** Turnover of amyloid- $\beta$  (A $\beta$ )42 is accelerated in individuals with amyloidosis. The accumulation of  $^{13}\text{C}$ -leucine in A $\beta$  peptides, termed the mole fraction labelled (MFL), was normalized to the plasma  $^{13}\text{C}$ -leucine plateau MFL for each person and averaged for 46 individuals without amyloidosis (age  $\pm$  1 s.d.  $72.8 \pm 6.3$  years; part **a**) and 54 matched individuals with amyloidosis (age  $\pm$  1 s.d.  $73.6 \pm 6.9$  years; part **b**). Mean  $\pm$  95% CI error bars are shown for A $\beta$ 40 (green) and A $\beta$ 42 (red). A $\beta$ 42 shows identical kinetics to A $\beta$ 40 in amyloidosis-negative individuals but shows faster turnover (that is, an earlier peak) than A $\beta$ 40 in amyloidosis-positive individuals. A $\beta$  turnover slows with ageing. Normalized MFLs for A $\beta$ 40 (part **c**) and A $\beta$ 42 (part **d**) were averaged for amyloidosis-negative individuals in three different age groups: <60 years (blue,  $n = 23$ ), 60–70 years (red,  $n = 27$ ) and >70 years (green,  $n = 28$ ). Turnover of A $\beta$  peptides declines with increasing age, as shown by successively later, broader and lower peaks. Similar age-related trends were found in amyloidosis-positive individuals (not shown). Data points in all four graphs were fitted to comprehensive compartmental models describing the time course of  $^{13}\text{C}$ -leucine A $\beta$  kinetics (solid lines). Adapted with permission from REF.<sup>8</sup>, Wiley-VCH.

changes in A $\beta$  production underpin the sleep-mediated changes in A $\beta$  concentration.

**Amyloid- $\beta$  SILK in human brain tissue.**

The increased clearance of soluble A $\beta$ 42 from the CSF seen in individuals with amyloid deposition suggests that this protein is being incorporated into amyloid plaques<sup>9</sup>. SILK studies in combination with nanoscale secondary ion MS (NanoSIMS), collectively termed SILK-SIMS, has been used to image  $^{13}\text{C}_6$ -leucine in post-mortem brain sections from patients with AD<sup>23</sup> (FIG. 4). This high-resolution technique quantified the amount of labelled A $\beta$  protein deposited in brain amyloid plaques in vivo during the interval between  $^{13}\text{C}_6$ -leucine administration and death (range 8 days to 4 years)<sup>23</sup>. The findings confirmed that labelled A $\beta$ 42 (and other A $\beta$  proteins) is incorporated into plaques over the course of several days after label administration, indicating that plaques are dynamic structures that continue to sequester newly synthesized A $\beta$  (that is,

the A $\beta$  produced during the labelling time window) rather than being fixed structures that remain unchanged in the brain for many years. Indeed, A $\beta$  sequestration was shown to be a highly active process. This promising result, albeit obtained in a small number of participants, has led to the accelerated launch of a hospice study to measure plaque dynamics in human brains using SILK-SIMS. This technique has great potential to quantify the dynamics of other proteins in a range of neurodegenerative conditions.

**Apolipoprotein E**

SILK studies of apolipoprotein E (ApoE) turnover in plasma and CSF have been conducted to investigate the risk of AD conferred by different ApoE isoforms<sup>10,24–26</sup>. All ApoE isoforms have similar turnover rates in CSF. In plasma, however, ApoE4 turnover is twofold faster than ApoE3 turnover, which is twofold faster than ApoE2 turnover<sup>26</sup>. SILK studies of brain homogenates from transgenic mice

that express human APOE showed that clearance of ApoE, but not clearance of A $\beta$ , was modulated by overexpression of LDLR (encoding the LDL receptor) and by knockout or overexpression of ABCA1 (encoding ATP-binding cassette A1)<sup>25</sup>. The A $\beta$  synthesis rate in these mice was not modulated by expression of any human ApoE isoform<sup>24</sup>, which is consistent with SILK findings in humans that A $\beta$  kinetics in CSF are not modified by ApoE isoforms<sup>15</sup>.

**Superoxide dismutase 1**

Heterozygous mutations in SOD1 are the cause of ~1–2% of amyotrophic lateral sclerosis (ALS) cases. SOD1 SILK studies can simultaneously quantify the turnover of both mutant and normal SOD1 in the same participant<sup>27</sup>. The motivation to develop this technology was driven by the recognition that SOD1 turnover rates might be particularly informative in the development of novel therapeutic strategies for ALS that focus on lowering levels of SOD1 mRNA. Improved understanding of SOD1 protein turnover in human CSF could inform the timing of CSF sampling in clinical trials of such agents and might improve estimation of the magnitude of the decrease in SOD1 levels.

SOD1 SILK requires a lengthy sampling protocol because the half-life of SOD1 in human CNS is ~25 days<sup>27</sup>. Studies of SOD1 turnover in CSF are ongoing in patients with ALS and known SOD1 mutations, patients with ALS without a known genetic cause and healthy controls. In mouse and rat models of ALS, SILK studies showed that measures of SOD1 synthesis responded earlier to treatment with RNA-lowering therapeutics than did the total concentration of SOD1 in CSF, suggesting that the changes in protein dynamics as measured by SILK might be promising early pharmacodynamic markers for RNA-targeted therapeutics<sup>28</sup>.

**Tau**

Along with amyloid plaques, tau aggregates (also known as neurofibrillary tangles) are a pathological hallmark of AD and other neurodegenerative diseases, collectively termed the tauopathies. Tauopathies are distinguished according to which tau isoforms are enriched in these aggregates, as differentiated by the number of repeats (R) in their microtubule-binding region: 3R in Pick disease, 4R in corticobasal degeneration and progressive supranuclear palsy and a mixture of 3R and 4R in AD tauopathies<sup>29</sup>. In addition to increased deposition of aggregated tau, patients with AD have increased CSF levels of total tau and specific phosphorylated tau (p-tau)

species. Therefore, tau SILK studies were implemented to test the hypothesis that the increased CSF levels of tau and/or p-tau observed in these patients are due to changes in tau production or clearance rates.

Similarly to SOD1 SILK<sup>27</sup>, lengthy sampling protocols are required for SILK studies of tau, which has a CNS half-life of ~23 days<sup>30</sup>. To reduce the burden on study participants, 8h, 16h or 24h intravenous infusion protocols were used and CSF samples were obtained at 4–5 follow-up visits scheduled over several months. Data from 24 participants with and without amyloidosis suggest that tau clearance is not altered by the presence of tau aggregates, as measured by <sup>18</sup>F-flortaucipir PET, although the tau production rate is doubled in the presence of amyloid deposition<sup>30</sup>.

SILK studies have also been used to study tau kinetics in human iPSC-derived neurons. In vitro SILK studies offer several advantages over in vivo models, including increased label uptake, increased sampling frequency, ease of genetic and pharmacological intervention and access to intracellular compartments (TABLE 1). In cell lysates, >15 tau peptides incorporate <sup>13</sup>C<sub>6</sub>-leucine, including 3R tau, 4R tau and p-tau. Tau truncation profiles found in iPSC-derived neurons and their culture media were similar to those found in brain and CSF, respectively. Despite this similarity, tau peptides measured in iPSC-derived neurons exhibited much shorter half-lives than those of the same peptides measured in human CSF (6 days versus 23 days). This observation could be explained by the complex interplay of multiple cell types in the CNS (including glia and different neuronal subtypes) and the effects of protein transport from the brain into CSF on tau kinetics. Other in vitro SILK studies also demonstrated that the release of full-length tau into the CSF occurred with no time delay, whereas truncated forms of tau were released into the CSF after 3 days. This observation adds to prior evidence for an active truncation and secretion mechanism for tau<sup>27,31</sup>. Tau isoforms that are prone to aggregation might show increased turnover rates: 4R-tau isoforms and some types of p-tau exhibited faster turnover than 3R-tau isoforms or non-phosphorylated tau.

Tau SILK studies have considerable potential to advance our understanding of tau metabolism in health and disease and to provide tools for investigating the mechanisms of novel tau-targeted therapies<sup>32</sup>. These in vitro SILK studies might involve iPSC-derived neurons and other cell types derived from patients with

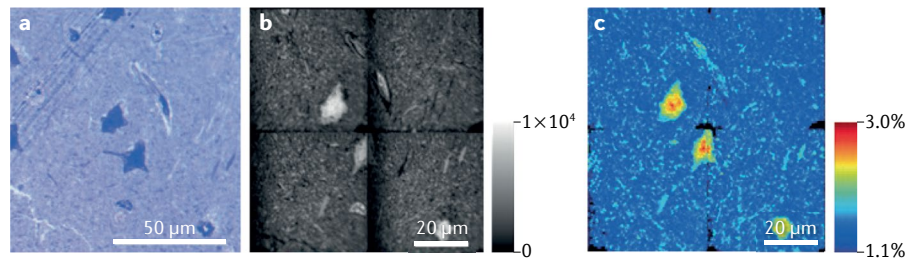


**Fig. 4 | Imaging scans showing incorporation of a stable isotope tracer into living brain tissue.** Stable isotope labelling kinetics (SILK)-secondary ion mass spectrometry (SIMS) studies enable quantitative imaging of stable isotopes such as <sup>13</sup>C at high spatial resolution (50–100 nm or <1 μm<sup>3</sup>, much smaller than a single cell). The technique is capable of mass resolution between <sup>13</sup>C and <sup>12</sup>CH (13.00159 Da versus 13.00605 Da) or <sup>13</sup>C<sup>14</sup>N and <sup>12</sup>C<sup>14</sup>N (27.00276 Da versus 26.99644 Da). SILK-SIMS is also a high-sensitivity technique; <1% enrichment can be detected. By contrast, PET imaging obtains only average measurements at ~1 cm resolution, and the resolution of confocal microscopy is ~0.5–1.0 μm. The result is a nanometre-level histological map of in situ incorporation of a stable isotope tracer. **a** | Optical image of neurons stained with toluidine blue (magnification ×40). **b** | <sup>12</sup>C<sup>14</sup>N ion map of the same field of view shown in panel **a**. Imaging carbon as cyanide ions (CN<sup>-</sup>) results in improved image quality and contrast owing to the increased count rate per pixel attributable to its ionization. In addition, measuring carbon as CN<sup>-</sup> produces an enhanced image of biological material owing to the abundance of carbon, nitrogen and C–N bonds, which almost entirely removes the carbon-rich and nitrogen-poor signals contributed by the embedding media. **c** | A false-colour <sup>13</sup>C<sup>14</sup>N and <sup>12</sup>C<sup>14</sup>N ion map showing the distribution of <sup>13</sup>C in the sample. The natural abundance of <sup>13</sup>C is 1.1%.

mutations linked to AD and frontotemporal dementia, in combination with advanced cell culture systems (including transdifferentiation, organoids, long-term culture and co-culture) and genome-editing techniques<sup>32</sup>.

### Potential applications of SILK

In this section, we consider potential practical advantages of SILK over techniques based on static biomarkers and hypothetical applications of SILK technology for probing specific aspects of neurodegeneration. Much work remains to be done as very few data currently exist about the turnover of the proteins mentioned in this section.

#### Kinetic versus static biomarkers

The concentration of a protein biomarker measured at a given time point in a biological fluid is an example of a static biomarker. The equilibrium of such static biomarkers could be affected by various factors, including increased protein production and/or secretion, increased protein release in response to a stimulus such as injury or disruption of cellular integrity or defective clearance from the biological fluid. By contrast, SILK provides dynamic measures of protein production and clearance that might provide a more detailed understanding of the actual mechanism or mechanisms underlying these changes in biomarker concentration. CSF tau levels offer a striking example of the advantages of dynamic biomarkers over static biomarkers<sup>30</sup>. The increased CSF tau concentration observed in patients with AD was initially

interpreted as resulting from the passive release of this protein by dying neurons<sup>33</sup>. By contrast, results from SILK studies suggest that the bulk of tau in human CSF is released by an active process that is stimulated by neuronal exposure to aggregated Aβ<sup>30</sup>.

#### Presymptomatic diagnosis

In neurodegenerative diseases characterized by the accumulation of misfolded or otherwise defective proteins, altered production or clearance of a protein might be a trait (that is, lifelong) marker that precedes build-up of the protein in inclusions or aggregates. Informative changes in the turnover of such proteins might occur during the progression of disease that could be monitored using SILK. For example, during the progression of AD and other neurodegenerative diseases, increased secretion of a protein might be followed by a phase of decreased production due to the loss of viable neurons. Similarly, disease-stage-dependent changes in protein clearance could result in altered CSF or plasma concentrations. SILK studies could potentially identify the cause of such changes, and this information could lead to the identification of early biomarkers or drive the development of therapies specifically targeting either production or clearance<sup>32</sup>.

#### Correcting for interindividual variation

By determining the production and clearance rates of multiple proteins, SILK can assist in understanding normal interindividual differences in protein

Table 1 | Comparison of different SILK biological models

Characteristic	In vitro	In vivo	
	Cell models	Animal models	Humans
Study purpose	<ul style="list-style-type: none"> <li>Investigate protein metabolism in cells</li> <li>Evaluate the effect of disease-causing genetic mutations</li> <li>Measure the effects of post-translational modifications on protein kinetics</li> <li>Identify drug effects on protein kinetics</li> </ul>	<ul style="list-style-type: none"> <li>Assess drug engagement and effects on protein kinetics (preclinical phase)</li> <li>Evaluate differences between protein kinetics in various tissues</li> </ul>	<ul style="list-style-type: none"> <li>Investigate protein kinetics in human physiology and pathophysiology</li> <li>Assess target engagement of drugs in clinical trials</li> </ul>
Labelling	<ul style="list-style-type: none"> <li>Labelling up to 100% TTR provides full dynamic range of kinetic curves</li> <li>Cost-effective (low amounts of tracer required)</li> </ul>	<ul style="list-style-type: none"> <li>Short half-life proteins are efficiently labelled at 5–10% TTR via intraperitoneal injection (200 mg/kg)</li> <li>Long half-life proteins are efficiently labelled with ≤20% TTR via labelled chow, water or injection</li> </ul>	<ul style="list-style-type: none"> <li>Infusion and oral treatment durations are both protein-dependent (for example, tau infusion 2–4 mg/kg/h for 8–24 h or oral 1 g daily for 10 days)</li> <li>Short half-life proteins: can label ≤15% TTR</li> <li>Long half-life proteins: can label ≤1% TTR</li> </ul>
Sampling	<ul style="list-style-type: none"> <li>Supernatant collected during media exchange (no cell harvest required) enables secreted proteins to be analysed</li> <li>Cells can be collected as frequently as needed</li> <li>Less abundant proteins might require large cultures (larger wells or organoid cultures)</li> </ul>	<ul style="list-style-type: none"> <li>Tissues (for example, brain, spinal cord, liver) can be collected post-labelling</li> <li>Biofluids (CSF, interstitial fluid, plasma or serum) can be collected, but will require animal sacrifice for sufficient sample volumes</li> </ul>	<ul style="list-style-type: none"> <li>Short half-life proteins: catheter preferred to allow hourly CSF sampling (max time: 48 h)</li> <li>Long half-life proteins: serial lumbar punctures over a few weeks to months</li> <li>Plasma, urine and saliva offer flexible sampling with few regulatory restrictions</li> </ul>
Advantages	<ul style="list-style-type: none"> <li>Human cell lines can be obtained from individuals with disease-relevant genotypes via skin biopsy</li> <li>Genome editing can generate isogenic cell lines to remove variability</li> <li>Storage and expansion of cell lines allow for a virtually limitless supply of material</li> <li>Differentiation into multiple disease-relevant cell types (neurons, astrocytes and microglia) and co-culture models is possible</li> <li>Transdifferentiation of fibroblasts directly to neurons maintains molecular ageing signatures of participants</li> <li>Molecular mechanisms and kinetic responses to genetic and pharmacological manipulations can be easily investigated in great detail</li> <li>Detailed kinetic modelling of tracer and tracee due to highly efficient label incorporation and frequent sampling</li> <li>Enables comparison of intracellular and extracellular protein kinetics</li> </ul>	<ul style="list-style-type: none"> <li>High labelling efficiency</li> <li>Easy access to tissue for kinetic monitoring</li> <li>High protein content in tissue enables post-translational modification monitoring</li> <li>Suitable model to study drug engagement in preclinical phase</li> </ul>	<ul style="list-style-type: none"> <li>Most relevant model to study human biology and abnormal protein kinetics in neurodegenerative diseases</li> <li>Suitable technique to monitor target engagement in clinical trials</li> <li>Kinetic data can improve how established static biomarkers are interpreted</li> <li>Could provide insight into the role of target proteins in disease aetiology, progression and severity</li> </ul>
Disadvantages	<ul style="list-style-type: none"> <li>Neuronal cultures lack the different neuronal subtypes, non-neuronal cells and vasculature that contribute to pathology in vivo, thus in vitro systems only partially recapitulate in vivo situations</li> <li>iPSC neurons and glia are more representative of immature cultures than adult cultures</li> <li>Interpatient and inpatient heterogeneity of iPSCs can result in high variability and require multiple cell lines and/or isogenic cell lines to compare genotypes</li> </ul>	<ul style="list-style-type: none"> <li>Limited CSF volume: longitudinal collection from a murine model not possible and potentially problematic for LC-MS analysis</li> <li>Rat CSF volumes more suitable than mouse; however, rat disease models are less defined</li> <li>Disease model protein kinetics in animals may not be fully translatable to humans or human pathologies</li> </ul>	<ul style="list-style-type: none"> <li>Requires hospital stay for duration of intravenous labelling study</li> <li>Although safe, lumbar puncture can cause discomfort for some patients and requires trained practitioner</li> <li>Infusion-grade tracer must meet pharmaceutical criteria</li> <li>Large doses required for sufficient CNS labelling</li> <li>High labelling costs limit study design</li> <li>Limited sampling frequency</li> <li>Tissue availability depends on donations or surgery</li> <li>Monitoring low-abundance proteins requires high-resolution MS and/or large sample volumes</li> </ul>

CSF, cerebrospinal fluid; iPSCs, induced pluripotent stem cells; LC, liquid chromatography; MS, mass spectroscopy; SILK, stable isotope labelling kinetics; TTR, tracer:tracee ratio.

concentrations. A number of additional aspects should be explored, such as changes in overall CSF production and clearance rates associated with dysfunction of the choroid plexus<sup>34</sup> or blood–brain barrier<sup>35</sup>, which could affect both CSF biomarker concentrations and SILK data on individual proteins. For example, using SILK studies to measure the production and clearance rates of choroid-plexus-derived molecules could potentially lead to the quantitative measurement of CSF dynamics. Furthermore, paired measurements of turnover rates in CSF and blood might yield information about the intrathecal versus peripheral production of a biomolecule.

#### Measuring target engagement

SILK might be useful to confirm target engagement of a new treatment, for example, by detecting alterations in the production rate of a specific protein in CSF or blood in response to a putative disease-modifying therapy. Such changes in protein kinetics might occur before a change in the steady-state protein concentration is observed<sup>32</sup>. This application of SILK studies is particularly important in neurodegenerative diseases, in which a reservoir of the protein in brain tissue might affect its CSF or plasma concentration. Refined protein turnover measurements might result in increased statistical power (and consequently the need to recruit fewer patients) in clinical trials of new treatments.

#### Probing synaptic degeneration

Synaptic impairment and synapse loss are early features of neurodegenerative diseases, including AD, that occur before frank neuronal degeneration<sup>36</sup>. This observation has prompted the investigation of synaptic proteins as early-stage biomarkers. Neurogranin, a dendritic protein enriched in neurons, is the best-established CSF biomarker of synapse loss or dysfunction associated with AD<sup>37–39</sup>. SILK could help to clarify whether increases in the CSF concentration of synaptic markers reflect synaptic degeneration and/or injury or increased marker secretion triggered by the synaptic dysfunction or altered neuronal activity patterns; if the increase in CSF concentration of neurogranin in patients with AD is caused by accelerated biomarker production, levels of labelled protein would rise, whereas if the increase is attributable to the release of pre-existing synaptic proteins from dying synapses, only the level of unlabelled protein would increase.

#### Probing axonal degeneration

Neurofilament light polypeptide (NFL), a microfilament component of the neuronal cytoskeleton, is a promising protein biomarker of axonal damage in a range of diseases. NFL levels in CSF are elevated in several neurodegenerative diseases<sup>40</sup> and in active neuroinflammation<sup>41</sup>. CSF and serum NFL concentrations are increased after traumatic brain injury (TBI) and peak at 144 h after TBI<sup>42</sup>. This delay could perhaps be explained by a long half-life of NFL. In mice, the results of a single study suggest that the half-life of NFL could be as long as 50 days<sup>42</sup>, but NFL kinetics in human CSF and serum are currently unknown. Therefore, NFL-SILK could be used to elucidate the meaning of these elevated NFL levels — specifically whether such elevations relate to passive release of NFL by damaged axons or upregulated production and secretion of this protein reflecting attempted axonal regeneration. Protein kinetic information is critical to accurately interpret changes in levels of this biomarker and to determine whether an elevated NFL concentration has the same meaning across different neurodegenerative and neuroinflammatory diseases.

#### Probing neuroinflammation

A substantial body of evidence indicates that neuroinflammation plays an important and early part in neurodegeneration. For example, the genes *TREM2* (REF.<sup>43</sup>) and *CD33* (REF.<sup>44</sup>) (both of which encode immune receptors) are associated with AD and other neurodegenerative diseases. Triggering receptor expressed on myeloid cells 2 (*TREM2*) is a type 1 transmembrane protein expressed on the surface of microglia. The ectodomain of *TREM2* is proteolytically cleaved and released into the extracellular space as secreted *TREM2* (s*TREM2*), which can be measured in CSF. In patients with AD, CSF levels of s*TREM2* increase later than alterations in CSF levels of A $\beta$  or tau, but still before the onset of cognitive symptoms<sup>45</sup>. The function or functions of s*TREM2* are unknown, but SILK studies might be able to determine whether the rise in s*TREM2* concentration in CSF reflects increased proteolytic cleavage of *TREM2* (which would be shown by reduced labelling) or increased production (which would be shown by increased labelling).

#### Proteomics

Finally, proteins or peptides labelled with stable isotopes can be detected and quantified using non-targeted (shotgun) proteomics. This bottom-up approach

relies on the proteolytic digestion of all proteins in a sample followed by separation of the resulting peptides using high-performance liquid chromatography and their identification using tandem MS. With optimal pre-analytic fractionation of the digested peptides, up to 2,630 different proteins can be identified in normal CSF<sup>46</sup>. Preliminary SILK studies, which used LysC or trypsin to digest and fractionate CSF samples followed by quadrupole time-of-flight (Q-TOF) MS, identified a total of 6,398 peptides corresponding to 1,226 proteins<sup>47</sup>. Of these peptides, 4,528 (corresponding to 1,064 proteins) contained leucine and were therefore susceptible to <sup>13</sup>C<sub>6</sub>-leucine labelling. About 10% of the labelled peptides, corresponding to >200 proteins, showed sufficient incorporation of <sup>13</sup>C<sub>6</sub>-leucine to enable the ratio of labelled to unlabelled peptide to be quantified<sup>47</sup>. This capacity of SILK studies to analyse many proteins in parallel can provide information on multiple relevant metabolic and pathophysiological pathways. In addition, by serial analysis of multiple peptides belonging to a single protein, SILK studies can also access the differential behaviours of individual protein domains or features (such as amino-terminal or carboxy-terminal domains) or different isoforms of the same protein (such as ApoE2, ApoE3 and ApoE4).

The analysis of protein kinetics in CSF samples from multiple patients requires a sophisticated bioinformatics pipeline with mathematical modelling to extract different turnover patterns. However, this approach creates an opportunity to discover new dynamic biomarkers, which might be more useful than existing static markers.

#### Conclusions

SILK is a valuable method for quantifying the rates of production and clearance of specific proteins in vitro and in vivo in different compartments including CSF, blood and brain tissue. If applied to both blood and CSF, SILK studies can also provide relevant information on the movement of proteins between these compartments. Such information can be used to explore the function of the blood–brain barrier and blood–CSF barrier, which is believed to be important in several disorders and neurodegenerative diseases.

To date, SILK studies have determined the turnover rates of A $\beta$ , ApoE, tau and SOD1 in the human CNS and described altered patterns of A $\beta$  and tau metabolism in AD. SILK studies have also shown that sleep deprivation and advanced age influence A $\beta$  clearance. This method



offers the potential to probe other disease pathways in neurodegeneration and may be useful to demonstrate target engagement by putative disease-modifying therapies. Nonetheless, the widespread use of SILK studies in humans is still limited by the high cost of infusion-grade stable isotopes, the availability of suitable MS facilities and the considerable clinical time and effort associated with conducting such studies (TABLE 1). However, several important research questions can be addressed only by SILK studies, and sharing clinical and bench protocols as well as resources such as labelled amino acids will help to overcome or mitigate these limitations.

Ross W. Paterson<sup>1\*</sup>, Audrey Gabelle<sup>2,3,4</sup>, Brendan P. Lucey<sup>5</sup>, Nicolas R. Barthelemy<sup>5</sup>, Claire A. Leckey<sup>6</sup>, Christophe Hirtz<sup>2,3,4</sup>, Sylvain Lehmann<sup>2,3,4</sup>, Chihiro Sato<sup>10,5</sup>, Bruce W. Patterson<sup>7</sup>, Tim West<sup>10,9</sup>, Kevin Yarasheski<sup>8</sup>, Jonathan D. Rohrer<sup>1</sup>, Norelle C. Wildburger<sup>10,5</sup>, Jonathan M. Schott<sup>10,1</sup>, Celeste M. Karch<sup>10,9</sup>, Selina Wray<sup>6</sup>, Timothy M. Miller<sup>5</sup>, Donald L. Elbert<sup>10</sup>, Henrik Zetterberg<sup>1,11,12,13</sup>, Nick C. Fox<sup>1</sup> and Randall J. Bateman<sup>5</sup>

<sup>1</sup>Dementia Research Centre, Department of Neurodegeneration, University College London (UCL) Institute of Neurology, London, UK.

<sup>2</sup>Department of Neurology, Memory Research and Resources Centre, Centre Hospitalier Universitaire (CHU), Montpellier, France.

<sup>3</sup>University of Montpellier, Campus Universitaire du Triolet, Montpellier, France.

<sup>4</sup>INSERM U1163, Institut de Médecine Régénérative, Saint Eloi Hospital, Montpellier, France.

<sup>5</sup>Department of Neurology, Washington University School of Medicine, St Louis, MO, USA.

<sup>6</sup>Department of Neurodegenerative Disease, University College London (UCL) Institute of Neurology, London, UK.

<sup>7</sup>Department of Medicine, Washington University School of Medicine, St Louis, MO, USA.

<sup>8</sup>C2N Diagnostics, Center for Emerging Technologies, St Louis, MO, USA.

<sup>9</sup>Department of Psychiatry, Washington University, St Louis, MO, USA.

<sup>10</sup>Department of Neurology, Dell Medical School, University of Texas at Austin, Austin, TX, USA.

<sup>11</sup>UK Dementia Research Institute at University College London (UCL), London, UK.

<sup>12</sup>Clinical Neurochemistry Laboratory, Sahlgrenska University Hospital, Mölndal, Sweden.

<sup>13</sup>Department of Psychiatry and Neurochemistry, Institute of Neuroscience and Physiology, Sahlgrenska Academy at University of Gothenburg, Mölndal, Sweden.

\*e-mail: r.paterson@ucl.ac.uk

<https://doi.org/10.1038/s41582-019-0222-0>

Published online 20 June 2019

1. Wilkinson, D. J. Historical and contemporary stable isotope tracer approaches to studying mammalian protein metabolism. *Mass Spectrom. Rev.* **37**, 57–80 (2018).
2. Gregg, C. T. et al. Substantial replacement of mammalian body carbon with carbon-13. *Life Sci.* **13**, 775–782 (1973).

3. Haass, C. & Selkoe, D. J. Cellular processing of beta-amyloid precursor protein and the genesis of amyloid beta-peptide. *Cell* **75**, 1039–1042 (1993).
4. Xie, L. L. et al. Sleep drives metabolite clearance from the adult brain. *Science* **342**, 373–377 (2013).
5. Roberts, K. F. et al. Amyloid- $\beta$  efflux from the central nervous system into the plasma. *Ann. Neurol.* **76**, 837–844 (2014).
6. Eckman, E. A. & Eckman, C. B. A $\beta$ -degrading enzymes: modulators of Alzheimer's disease pathogenesis and targets for therapeutic intervention. *Biochem. Soc. Trans.* **33**, 1101–1105 (2005).
7. Da Mesquita, S. et al. Functional aspects of meningeal lymphatics in ageing and Alzheimer's disease. *Nature* **560**, 185–191 (2018).
8. Patterson, B. W. et al. Age and amyloid effects on human central nervous system amyloid-beta kinetics. *Ann. Neurol.* **78**, 439–453 (2015).
9. Wildsmith, K. R. et al. In vivo human apolipoprotein E isoform fractional turnover rates in the CNS. *PLoS ONE* **7**, e38013 (2012).
10. Potter, R. et al. Increased in vivo amyloid- $\beta$ 42 production, exchange, and loss in presenilin mutation carriers. *Sci. Transl. Med.* **5**, 189ra77 (2013).
11. Bateman, R. J. et al. A  $\gamma$ -secretase inhibitor decreases amyloid- $\beta$  production in the central nervous system. *Ann. Neurol.* **66**, 48–54 (2009).
12. Lucey, B. P. et al. Effect of sleep on overnight cerebrospinal fluid amyloid  $\beta$  kinetics. *Ann. Neurol.* **83**, 197–204 (2018).
13. Bateman, R. J. et al. Human amyloid- $\beta$  synthesis and clearance rates as measured in cerebrospinal fluid in vivo. *Nat. Med.* **12**, 856–861 (2006).
14. Mawuenyega, K. G. et al. Decreased clearance of CNS  $\beta$ -amyloid in Alzheimer's disease. *Science* **330**, 1774 (2010).
15. Dobrowolska, J. A. et al. CNS amyloid- $\beta$ , soluble APP- $\alpha$  and  $\beta$  kinetics during BACE inhibition. *J. Neurosci.* **34**, 8336–8346 (2014).
16. Cook, J. J. et al. Acute  $\gamma$ -secretase inhibition of nonhuman primate CNS shifts amyloid precursor protein (APP) metabolism from amyloid- $\beta$  production to alternative APP fragments without amyloid- $\beta$  rebound. *J. Neurosci.* **30**, 6743–6750 (2010).
17. Ovod, V. et al. Amyloid  $\beta$  concentrations and stable isotope labeling kinetics of human plasma specific to central nervous system amyloidosis. *Alzheimers Dement.* **13**, 841–849 (2017).
18. Alzforum. Finally a blood test for Alzheimer's? Series — Alzheimer's Association International Conference 2017: part 1 of 16. *Alzforum* <https://www.alzforum.org/news/conference-coverage/finally-blood-test-alzheimers> (2017).
19. Kang, J. E. et al. Amyloid- $\beta$  dynamics are regulated by orexin and the sleep-wake cycle. *Science* **326**, 1005–1007 (2009).
20. Huang, Y. F. et al. Effects of age and amyloid deposition on A $\beta$  dynamics in the human central nervous system. *Arch. Neurol.* **69**, 51–58 (2012).
21. Lucey, B. P. & Bateman, R. J. Amyloid- $\beta$  diurnal pattern: possible role of sleep in Alzheimer's disease pathogenesis. *Neurobiol. Aging* **35**, S29–S34 (2014).
22. Wildburger, N. C. et al. Amyloid- $\beta$  plaques in clinical Alzheimer's disease brain incorporate stable isotope tracer in vivo and exhibit nanoscale heterogeneity. *Front. Neurol.* **9**, 169 (2018).
23. Castellano, J. M. et al. Human apoE isoforms differentially regulate brain amyloid- $\beta$  peptide clearance. *Sci. Transl. Med.* **3**, 89ra57 (2011).
24. Basak, J. M. et al. Measurement of apolipoprotein E and amyloid  $\beta$  clearance rates in the mouse brain using bolus stable isotope labeling. *Mol. Neurodegener.* **7**, 14 (2012).
25. Baker-Nigh, A. T. et al. Human central nervous system (CNS) apoE isoforms are increased by age, differentially altered by amyloidosis, and relative amounts reversed in the CNS compared with plasma. *J. Biol. Chem.* **291**, 27204–27218 (2016).
26. Crisp, M. J. et al. In vivo kinetic approach reveals slow SOD1 turnover in the CNS. *J. Clin. Invest.* **125**, 2772–2780 (2015).
27. Self, W. K. et al. Protein production is an early biomarker for RNA-targeted therapies. *Ann. Clin. Transl. Neurol.* **5**, 1492–1504 (2018).
28. Buee, L. et al. Tau protein isoforms, phosphorylation and role in neurodegenerative disorders. *Brain Res. Brain Res. Rev.* **33**, 95–130 (2000).
29. Sato, C. et al. Tau kinetics in neurons and the human central nervous system. *Neuron* **97**, 1284–1298 (2018).
30. Karch, C. M., Jeng, A. T. & Goate, A. M. Extracellular tau levels are influenced by variability in tau that is associated with tauopathies. *J. Biol. Chem.* **287**, 42751–42762 (2012).
31. Pooler, A. M. et al. Physiological release of endogenous tau is stimulated by neuronal activity. *EMBO Rep.* **14**, 389–394 (2013).
32. Blennow, K. et al. Cerebrospinal fluid and plasma biomarkers in Alzheimer disease. *Nat. Rev. Neurol.* **6**, 131–144 (2010).
33. Gonzalez-Marrero, I. et al. Choroid plexus dysfunction impairs beta-amyloid clearance in a triple transgenic mouse model of Alzheimer's disease. *Front. Cell Neurosci.* **9**, 17 (2015).
34. Zlokovic, B. V. Cerebrovascular effects of apolipoprotein E implications for Alzheimer disease. *JAMA Neurol.* **70**, 440–444 (2013).
35. Selkoe, D. J. Alzheimer's disease is a synaptic failure. *Science* **298**, 789–791 (2002).
36. Hellwig, K. et al. Neurogranin and YKL-40: independent markers of synaptic degeneration and neuroinflammation in Alzheimer's disease. *Alzheimers Res. Ther.* **7**, 74 (2015).
37. Kester, M. I. et al. Neurogranin as a cerebrospinal fluid biomarker for synaptic loss in symptomatic Alzheimer disease. *JAMA Neurol.* **72**, 1275–1280 (2015).
38. Kvarnstrom, H. et al. Characterization of the postsynaptic protein neurogranin in paired cerebrospinal fluid and plasma samples from Alzheimer's disease patients and healthy controls. *Alzheimers Res. Ther.* **7**, 40 (2015).
39. Rosengren, L. E. et al. Neurofilament protein levels in CSF are increased in dementia. *Neurology* **52**, 1090–1093 (1999).
40. Kuhle, J. et al. Blood neurofilament light chain levels are elevated in multiple sclerosis and correlate with disease activity [abstract 249]. *Mult. Scler.* **22**, S828 (2016).
41. Zetterberg, H. et al. Neurochemical aftermath of amateur boxing. *Arch. Neurol.* **63**, 1277–1280 (2006).
42. Millecamps, S. et al. Conditional NF-L transgene expression in mice for in vivo analysis of turnover and transport rate of neurofilaments. *J. Neurosci.* **27**, 4947–4956 (2007).
43. Guerreiro, R. & Hardy, J. *TREM2* and neurodegenerative disease. *N. Engl. J. Med.* **369**, 1569–1570 (2013).
44. Griciuc, A. et al. Alzheimer's disease risk gene *CD33* inhibits microglial uptake of amyloid beta. *Neuron* **78**, 631–643 (2013).
45. Suarez-Calvet, M. et al. sTREM2 cerebrospinal fluid levels are a potential biomarker for microglia activity in early-stage Alzheimer's disease and associate with neuronal injury markers. *EMBO Mol. Med.* **8**, 466–476 (2016).
46. Schutzer, S. E. et al. Establishing the proteome of normal human cerebrospinal fluid. *PLoS ONE* **5**, e10980 (2010).
47. Lehmann, S. et al. Stable isotope labeling by amino acid in vivo (SILAV): a new method to explore protein metabolism. *Rapid. Commun. Mass Spectrom.* **29**, 1917–1925 (2015).

**Acknowledgements**

R.W.P. is supported by a UK National Institute for Health Research (NIHR) academic clinical lectureship. H.Z. is a Wallenberg Academy Fellow and is supported by grants from the Swedish Research Council, the European Research Council, the Olav Thon Foundation and the UK Dementia Research Institute at University College London (UCL). A.G., C.H. and S.L.'s stable isotope labelling kinetics (SILK) work is supported by the French 2010 National Programme Hospitalier de Recherche Clinique (PHRC) 'ProMara', Direction de l'Hospitalisation et de l'Organisation des Soins (DHOS). S.W. is supported by an Alzheimer's Research UK Senior Research Fellowship (ARUK-SRF2016B-2). B.P.L. is supported by a grant from the US National Institute on Aging (K76 AG054863). T.M.'s SILK studies are supported by US NIH grant R01-NS098716-01. C.M.K. is supported by NIH grant K01AG046374. N.C.F. acknowledges support from the NIHR UCL Hospitals Biomedical Research Centre, the Leonard Wolfson Experimental Neurology Centre and the UK Dementia Research Institute at UCL. R.J.B.'s SILK work was supported by the BrightFocus Foundation (grant A20143845), Tau SILK Consortium (AbbVie, Biogen and Eli Lilly), NIH grant R01-NS095773, MetLife Foundation, Alzheimer's Association Zenith Award Grant (institution grant #3856-80569), NIH (R01NS065667) and the Cure Alzheimer's Fund.

**Author contributions**

R.W.P., A.G., B.P.L., N.R.B., C.A.L., S.L., C.S., B.W.P., T.W., K.Y., J.D.R., N.C.W., J.M.S., T.M., D.L.E., H.Z., N.C.F. and R.J.B. researched data for the article. R.W.P., A.G., B.P.L., N.R.B., C.S., C.A.L., C.H., S.L., B.W.P., T.W., K.Y., N.C.W., D.L.E. and H.Z. wrote the first draft of the manuscript. R.W.P., J.D.R., J.M.S., S.W., N.C.F. and R.J.B. reviewed and critically edited the manuscript. All authors contributed substantially to discussions of the article content and to the review or editing of the manuscript before submission.

**Competing interests**

H.Z. declares that he has served on scientific advisory boards for Roche Diagnostics, Samumed, CogRx and Wave and is one of the founders of Brain Biomarker Solutions in Gothenburg, which is funded by GU Ventures (a Swedish government-owned company managed by the University of

Gothenburg); these activities are all unrelated to this article. R.J.B. declares that he, along with Washington University, has an equity ownership interest in C<sub>2</sub>N Diagnostics (a mass spectrometry-based biotechnology company that holds patents on the stable isotope labelling kinetics (SILK) technique in the United States and other countries) and receives royalties related to SILK and blood plasma assay technologies licensed by Washington University to C<sub>2</sub>N Diagnostics. R.J.B. declares that he receives income from C<sub>2</sub>N Diagnostics for serving on its scientific advisory board. B.W.P. declares that he receives consultancy fees from C<sub>2</sub>N Diagnostics. T.M. and R.J.B. have licensed superoxide dismutase 1 SILK to C<sub>2</sub>N Diagnostics. N.C.W. holds a patent for SILK studies utilizing nanoscale secondary ion mass spectroscopy. K.Y. and T.W. declare that they are employed by C<sub>2</sub>N Diagnostics. The other authors declare no competing interests.

**Publisher's note**

Springer Nature remains neutral with regard to jurisdictional claims in published maps and institutional affiliations.

**Supplementary information**

Supplementary information is available for this paper at <https://doi.org/10.1038/s41582-019-0222-0>.

**RELATED LINKS**

University College London (UCL) Dementia Research

Centre: <https://www.ucl.ac.uk/drc>

Washington University School of Medicine in St Louis

(WUSTL) Department of Neurology, Bateman Laboratory:

[https://neuro.wustl.edu/labs/bateman\\_r/Ongoing-Studies](https://neuro.wustl.edu/labs/bateman_r/Ongoing-Studies)